

# A 1.1-V 270- $\mu$ A Mixed-Signal Hearing Aid Chip

D. George Gata, *Member, IEEE*, Walter Sjrursen, *Member, IEEE*, James R. Hochschild, *Member, IEEE*, John W. Fattaruso, *Member, IEEE*, Lieyi Fang, *Member, IEEE*, Gerald R. Iannelli, Zhongnong Jiang, Charles M. Branch, *Member, IEEE*, James A. Holmes, Michael L. Skorcz, *Member, IEEE*, Eugene M. Petilli, Shuyou Chen, *Member, IEEE*, Gary Wakeman, David A. Preves, *Member, IEEE*, and William A. Severin

**Abstract**—This paper presents a single-chip mixed-signal IC for a hearing aid system. The IC consumes 270  $\mu$ A of supply current at a 1.1-V battery voltage. The presented circuit and architectural design techniques reduce the total IC power to 297  $\mu$ W, a level where up to 70 days of lifetime is achieved at 10 h/day for a small zinc-air battery. The measured input referred noise for the entire channel is 2.8  $\mu$ V<sub>rms</sub> and the average THD in the nominal operating region is 0.02%. The jitter for the on-board ring oscillator is 147 ps rms. The chip area is 12 mm<sup>2</sup> in a 0.6- $\mu$ m 3.3-V mixed-signal CMOS process.

**Index Terms**—Analog-to-digital conversion, digital filters, digital signal processing, digital-to-analog conversion, gain compression, hearing aid circuits, limiting, low power, low voltage, ring oscillator.

## I. INTRODUCTION

FIG. 1 SHOWS the signal path of the IC. All signal processing elements, with the exception of the microphone, receiver (earphone), and coupling and bypass capacitors are contained within the single mixed-signal IC. A preamplifier that includes gain compression limiting amplifies the output of the microphone. The limiter function prevents loud sounds from overloading the analog-to-digital converter (ADC), preventing distortion. A sigma-delta ADC outputs a bitstream at a rate of 1.28 MHz. This bit stream passes through a decimation filter and is down-sampled to a rate of 40 kHz. The digital signal processor operates on the 40-kHz rate data to perform the hearing aid signal-processing algorithm. The output of the digital signal processor drives a sigma-delta digital-to-analog converter (DAC) modulator where the signal is converted to a 2-b stream at a rate of 640 kHz. The output of the sigma-delta modulator goes through an H-bridge driver, which then drives the receiver, which converts the 2-b stream into an analog, acoustical signal. The digital signal processor needed to be optimized for low power and small size, yet had to provide a certain amount of flexibility. A general-purpose DSP core would provide the flexibility at the expense of power and

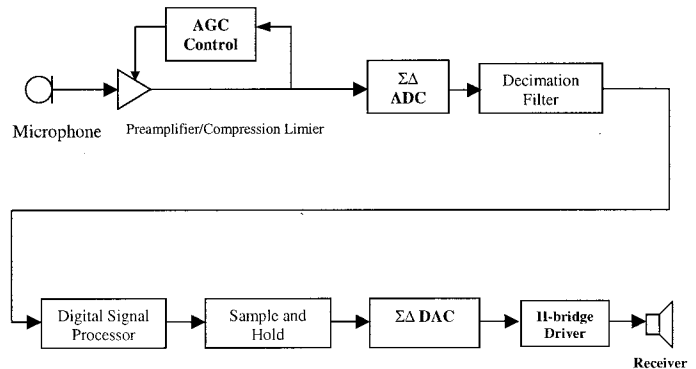


Fig. 1. Signal path block diagram.

size. A dedicated, hardwired digital signal processing circuit would consume minimal power and would be small, but would lack flexibility. The final design selection was a hardwired digital signal processing circuit with programmable parameters that adjust and configure the hearing aid signal-processing functions. The approach provides the needed flexibility without the penalties of a general-purpose DSP core.

The chip operates with a single-cell voltage supply, as low as 1.1 V. The 0.6- $\mu$ m 3.3-V CMOS IC process used includes a deep n-well layer essential for junction isolation of digital and analog sections. This layer also affords a vertical npn bipolar device in the input stage opamp to reduce  $1/f$  noise, as well as in the bandgap reference. Also available are a low-threshold voltage option for the MOS devices and EEPROM cells for prescription selection and analog trim functions. Both the input compression limiter (ICL) and the ADC use a locally boosted supply voltage to drive the nMOS analog switch gates. This work achieves 28 dB lower distortion while using one fifth the current consumption of previous low-power work [1], aided by process enhancements and new design techniques.

## II. ICL

A diagram of the ICL is shown in Fig. 2. After conversion from the single-ended microphone input by this stage, fully differential circuitry is employed throughout the analog blocks. A closed-loop architecture satisfies 0.03% input-stage harmonic distortion requirement and keeps static power consumption constant over all gain settings. Resistor taps and nMOS switches are provided for 83 gain steps of 0.5 dB, from  $-1$  to 40 dB. Input signals experience gain compression and release governed by four time constants. Relatively fast gain reduction and recovery occurs for brief and exceptionally high sound levels, whereas

Manuscript received March 31, 2002; revised August 1, 2002.

D. G. Gata, J. R. Hochschild, J. W. Fattaruso, L. Fang, Z. Jiang, C. M. Branch, J. A. Holmes, M. L. Skorcz, S. Chen, G. Wakeman, and W. A. Severin are with Texas Instruments Incorporated, Dallas, TX 75266 USA.

W. Sjrursen and D. A. Preves are with Songbird Hearing Inc., Cranbury, NJ 08512 USA.

G. R. Iannelli is with Sarnoff Corporation, Princeton, NJ 08543-5300 USA.

E. M. Petilli is with Intrinsic, Pittsford, NY 14534 USA.

Digital Object Identifier 10.1109/JSSC.2002.804328

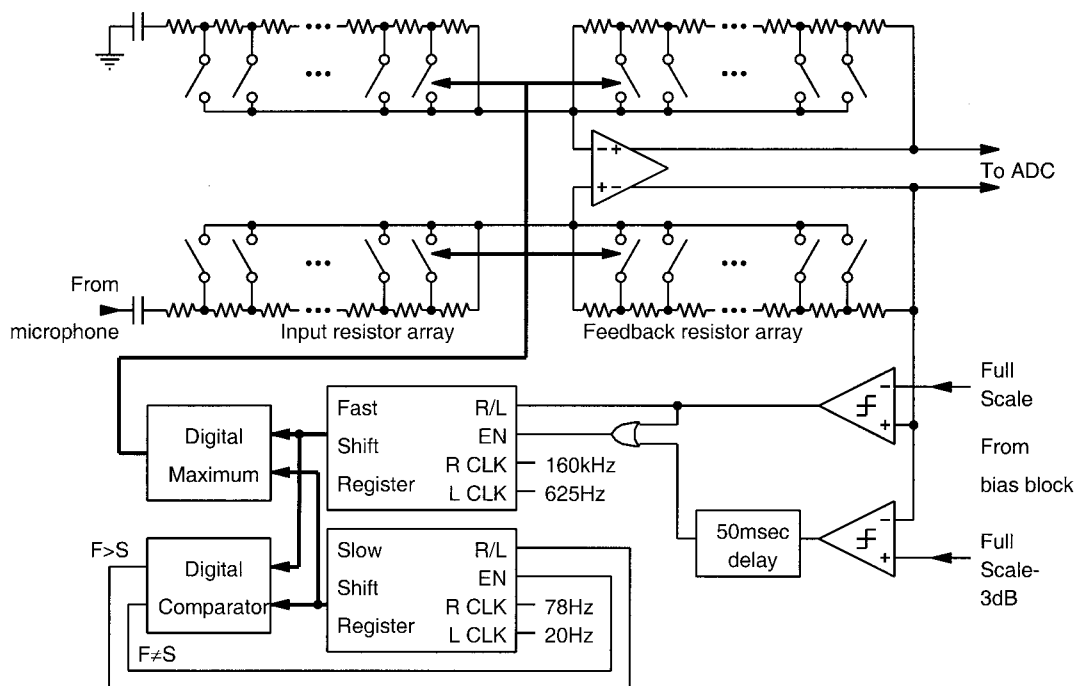


Fig. 2. ICL.

compression and release from sustained sound levels occur at significantly slower rates. A 3-dB hysteresis window inhibits changes in the gain setting for steady-state sound levels, preserving linearity. Even though the incremental resistance for each 0.5-dB gain step is nonuniform, almost all of the resistance required for each tap is realized with a varying number of unit resistors from an array of matched cells.

The bidirectional shift registers in Fig. 2 drive the resistor array switches without intervening decoder. These registers may change the state of only one switch per clock cycle, giving glitch-free gain steps. The Compare and Maximize functions are computed with a chain of simple bitwise gates. Closed-loop gain is reduced as “one” bits are shifted to the right in response to sound levels greater than full scale, and is increased as “zero” bits are shifted to the left during release. The first 57 steps of gain reduction are realized by taps on the feedback resistance, and the final 26 steps, for high sound levels, adjust the input resistance. This arrangement saves considerable bias current in the opamp output stage, since minimum load resistance is kept high, but still gives minimum noise with lower input resistances at high gain settings. The differential input resistors for high gain settings are 10 K $\Omega$  each, and the total feedback resistance available is 1 M $\Omega$ . Since the bandwidths are limited and the resistance values fairly high, the NMOS switches in the resistor arrays can be made large enough so that their channel resistance does not cause a gain error  $>0.1$  dB. Small stub resistors outside the array are then used on each tap to make up the difference between the nearest integer number of unit resistors and the nonuniform resistance required. With this layout, accurate logarithmic gain steps and accurate total gain are achieved. For further layout details, see [2].

Fig. 3 shows the ICL opamp schematic. The active part of the opamp is a fairly standard two-stage design. M1 and M2 are

the diff pair for the first stage, and Q1 and Q2 are their active loads. The choice of bipolar devices for the active loads reduces  $1/f$  noise. Then Q3 and Q4 are the amplifying devices for the second stage, with M3 and M4 their class-A active loads.  $C_c$  and  $R_c$  give pole-splitting compensation.  $R_{cm}$  and  $C_{cm}$  generate a common-mode output voltage level that is compared to the desired common-mode level  $V_{cm}$  by the diff pair of M9 and M10. Q6 and Q1–Q2 form a current mirror that completes the common-mode feedback loop. Q5 is in the circuit only to keep the  $V_{ds}$  of M9 matching the  $V_{ds}$  of M10 and minimize the offset in the M9 and M10 amplifiers. The base voltage of Q5 is fed to the gate of M14 because it was a convenient source of a bias voltage that is several hundred millivolts above the negative supply rail. There is no real signal being transmitted from Q5 to M14. M14 is a very long and thin device that is designed to just give a very small current (a fraction of a microamp) to M7 and M8. The actual drain current of M14 is not critical, and the gate voltage of M14 is not critical. Just enough current from M14 to sense when M5 is somewhere near the triode region is needed. When the opamp input common-mode voltage at the gates of M1, M2, M7, and M8 is in its proper operating range, slightly above mid-supply, then the drain current of M6 would be sufficient to pull the gates of M12 and M13 almost to the positive rail and M12 and M13 are off. However, when the input common-mode voltage is too high, and M5 is going into triode, then the  $V_{ds}$  across M6 is also very small. Then, whatever small drain current there is in M14 can pull the gate voltage of M12 and M13 low, turning them on. M12 and M13 then dumps some temporary bias current into the first stage, to substitute for the bias current into Q1 and Q2 that is no longer coming from M5 since it is in triode. This keeps the common-mode feedback loop active. Since there is overall resistive feedback around the opamp when the output common mode level is set by the feed-

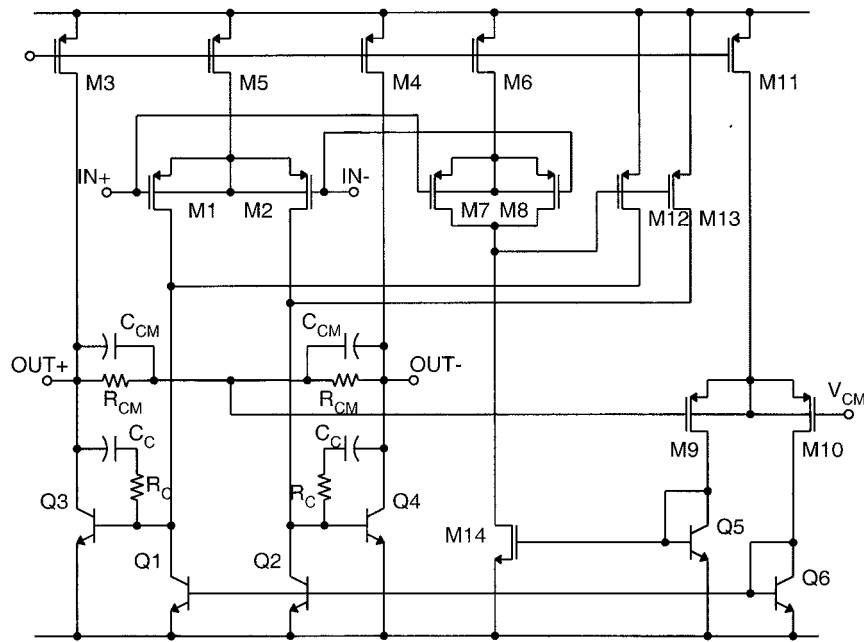


Fig. 3. ICL opamp schematic.

back loop, the input common mode is also quickly restored to its proper range and M12 and M13 are again turned off, leaving the opamp in its normal operating state. Without this circuitry, it is possible that the common-mode loop can settle in a stable operating point that drives both the output terminals to the positive rail caused by either an initial startup condition or a transient condition. M7, M8, and M6 are scaled down from M1, M2, and M3, to save power. M5 is 20 gate fingers, and M6 is a factor of 10 smaller. M1 and M2 have to be huge to reduce the opamp  $1/f$  noise to a very low level for the hearing aid, and they are 48 fingers, each  $52 \mu\text{m}$  wide by  $8 \mu\text{m}$  long. M7 and M8 are two fingers of  $4 \mu\text{m}$  by  $2 \mu\text{m}$ . Therefore, M7 and M8 are not exact scaled down replicas of M1 and M2, but for the operation of this circuit exact ratios are not necessary.

### III. SIGMA-DELTA ADC MODULATOR

The third-order  $\Sigma\Delta$  ADC modulator consists of a cascade of two single-bit stages, a second-order stage followed by a first-order stage [3]. The input sampling network for the first integrator is shown in Fig. 4. The use of a single pair of differential sampling capacitors  $C_S$  reduces the total input capacitance for a given  $kT/C$  noise budget and allows reduction of opamp power. An additional short clock phase  $\phi_3$  discharges these capacitors before each sample and erases the charge condition from the previous full-scale reference sample. This reduces the dynamic signal input charge required, eliminating an active buffer in preference to a simple passive RC anti-alias filter as shown. Furthermore, the switches that sample the reference voltage with a polarity that conveys the feedback digital bit  $D$  are arranged to hold both parasitic capacitances  $C_P$  discharged to ground except around time interval  $\phi_2$ . This suppresses a mechanism for data-dependent charge drain from the reference voltage and eliminates an active buffer for the reference. A simple RC filter from the battery supply, as shown, performs well as a reference

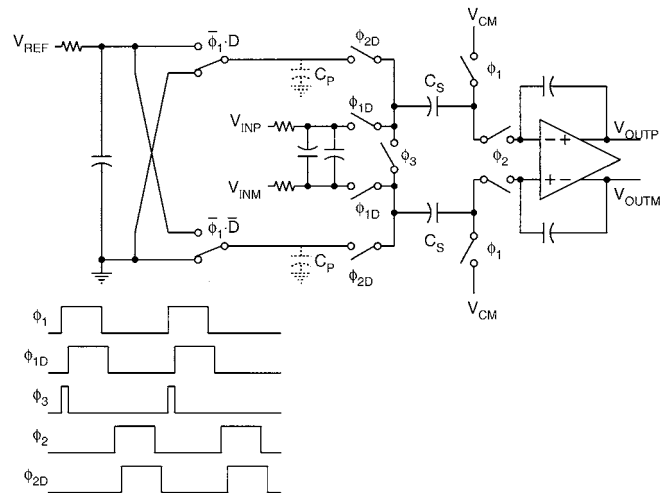


Fig. 4. First  $\Sigma\Delta$  ADC integrator.

supply in this system. Fig. 5 shows the measured performance of the ADC modulator operating at 1.28 MHz. It achieves a dynamic range of 87 dB unweighted from 100 Hz to 10 kHz and 92-dB signal to distortion, drawing a  $66\text{-}\mu\text{A}$  supply current. Following the ADC modulator, the decimation filter consists of a cascade of five polyphase finite impulse response (FIR) filters, each decimating by two with a transfer function  $H(z)$  of

$$H(z) = (1 + z^{-1})^4. \quad (1)$$

Droop from this filter is partially corrected by an FIR filter with a transfer function  $H_{\text{FIR}}(z)$  of

$$H_{\text{FIR}}(z) = 1 + (1 - z^{-2}) * 3/16. \quad (2)$$

The combined decimation plus droop correction filter draws an  $8\text{-}\mu\text{A}$  supply current.

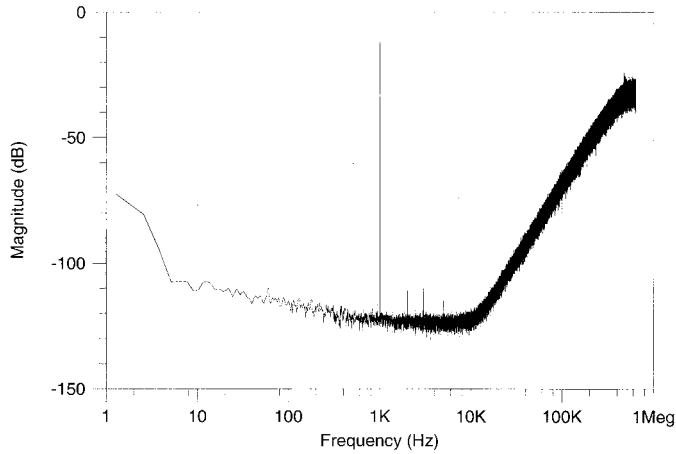


Fig. 5. Measured ADC spectrum.

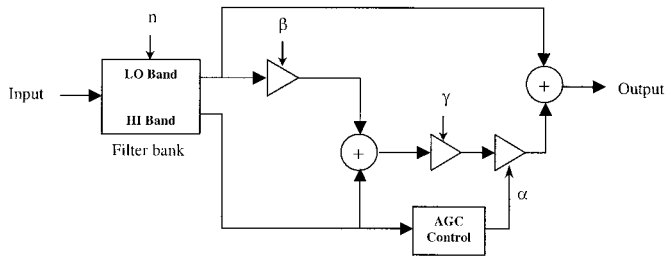


Fig. 6. Two-band AGC algorithm.

#### IV. DIGITAL SIGNAL PROCESSING SECTION

Fig. 6 shows a basic block diagram of the signal processing algorithm. The input signal is split into two frequency bands. Each subband is processed and then summed to provide a full bandwidth output. While the algorithm seems simple, the programmable parameters  $n$ ,  $\beta$ , and  $\gamma$  provide quite a bit of flexibility. Parameter  $n$  selects the transition characteristics between the low- and high-frequency bands. Parameter  $\beta$  enhances the low-frequency response by adding a fraction of the low-frequency signals through the high-frequency AGC channel. Parameter  $\gamma$  primarily controls the amount of high-frequency gain. The high-frequency channel has AGC. The AGC function is controlled by the signal from the high-band output of the filter bank and generates parameter  $\alpha$  controlling the AGC multiplier.

The filter is implemented as an FIR filter. This eliminates the finite word-length problems of infinite impulse response (IIR) filters such as overflow and limit cycles. With the FIR filter, the required word length at each part of the filter is deterministic. Unlike IIR filters where the word length is often made wider to minimize limit cycles, for example, the approach with FIR filters allows the word lengths to be optimized, resulting in less hardware, lower power, and smaller size. To further optimize the design, the FIR filter uses coefficients that are  $2^n$  values, and, in fact, all filter coefficients are 0.5. Multiplying by 0.5 is implemented by hardwired shifting of the signal bits and hence uses no power, or gates and is minimal size. The values of  $\beta$  and  $\gamma$  are also selected from  $2^n$  values and hence the  $\beta$ - and  $\gamma$ -multipliers are nothing more than a multiplexer implementing a selectable shifting function. With these optimizations, only one full multiplier is needed and is used only once per sample period. This is in contrast to a general-purpose DSP core and

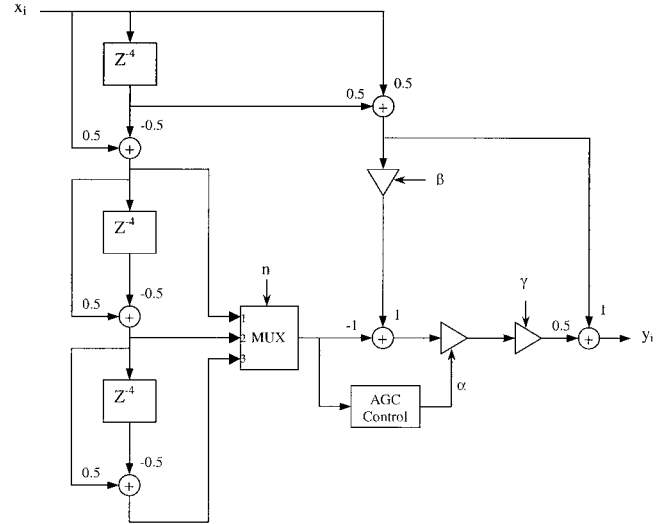


Fig. 7. Digital signal processor.

common DSP algorithms, where a single multiplier is used to perform many multiplications during each sample period.

The band splitting filter has been optimized for minimal circuitry, size, and power. Instead of using a more traditional low-pass and high-pass band splitting structure, a band-pass and notch-filter structure [4] was chosen. By selecting the appropriate sampling rate, the band-pass/notch structure provides psychoacoustically similar results to low-pass/high-pass structures. The advantage of the band-pass/notch structure is again a reduction in the power dissipation and physical size of the filter.

Originally, the digital filter was designed for a sample rate of 20 kHz. During the design of the IC, it was determined that, if the bitstream from the  $\Sigma\Delta$  ADC is downsampled to only 40 kHz, and each  $Z^{-1}$  delay in the filter was replaced with a  $Z^{-2}$  delay (i.e., a double delay), the power savings of the smaller decimation filter and the elimination of an interpolation filter in favor of a simple sample-and-hold circuit more than offset the added power of the additional delay elements. Therefore, the 40-kHz sample rate was used. Fig. 7 shows the final digital signal filter structure. The overall transfer function  $H_T(z)$  is given by

$$H_T(z) = \left[ (1 + 0.5\alpha\beta\gamma) (0.5 + 0.5z^{-4}) - (0.5\alpha\gamma) (0.5 - 0.5z^{-4})^n \right]. \quad (3)$$

Parameters  $n$ ,  $\beta$ , and  $\gamma$  are programmable. Parameter  $\alpha$  is determined by the AGC control circuit based on the level of the signal at the output of the multiplexer. Figs. 8–10 show the effect of each of the programmable parameters on the frequency response of the filter.

#### V. SIGMA-DELTA DAC

The sigma-delta DAC has a 20-b signed input at a sample rate of 40 kHz, ideally giving it a dynamic range of 120 dB. The dynamic range as designed was approximately 103 dB and the SNDR was approximately 80 db. The three-level fourth-order sigma-delta DAC minimizes power consumed in the output H-bridge driver, since most samples will be zero for the typical audio levels well below full scale. Increasing the quantization

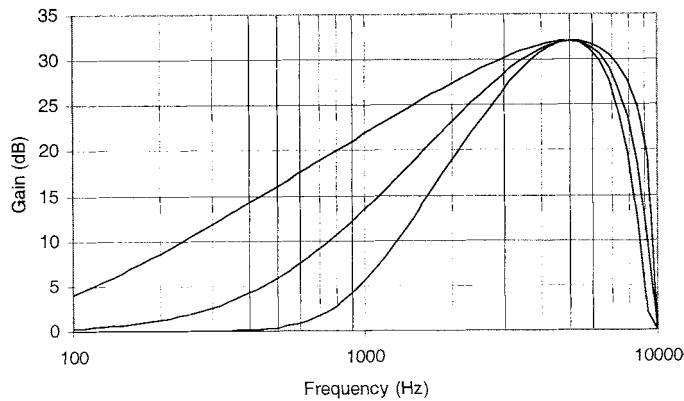
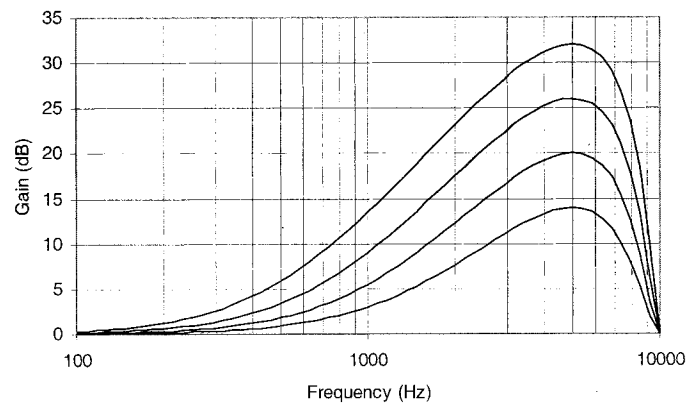
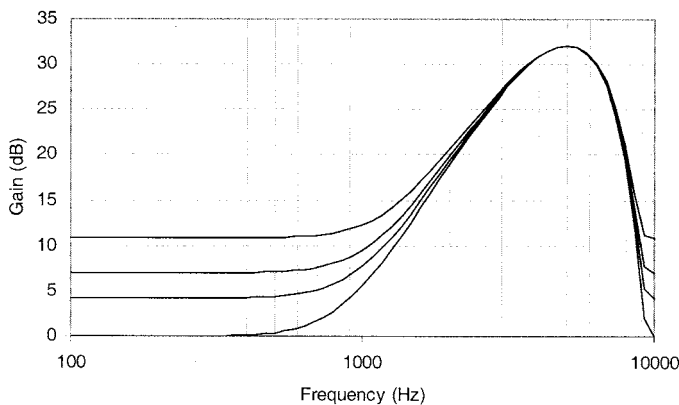
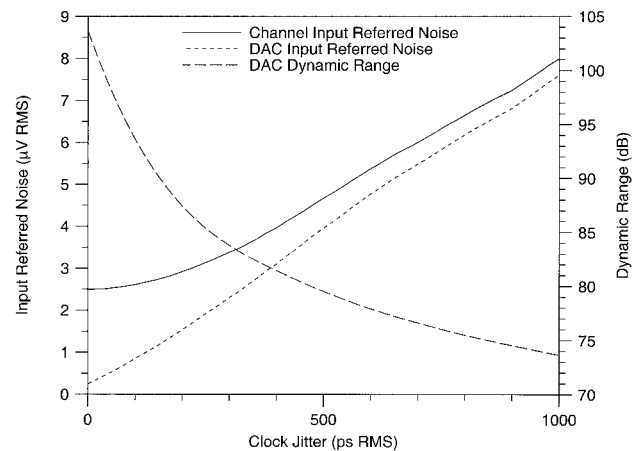
Fig. 8. Effect of varying  $n$  on a typical frequency response.Fig. 10. Effect of varying  $\gamma$  on a typical frequency response.Fig. 9. Effect of varying  $\beta$  on a typical frequency response.

Fig. 11. Simulated DAC performance versus clock jitter.

levels in the output of sigma-delta modulators improves the noise performance and stability of the loop. Typically, a two-level output is used since it is ideally linear and the accuracy of the quantization steps limits the sigma-delta performance. Since the speaker was to be driven differentially, we were able to sum the two ideally linear outputs in the load. This technique creates a three-level  $(-1, 0 +1)$  or 1.5-b highly linear output. In addition, since the required output power is usually very low, the output waveform is typically driven to zero with occasional single pulses of either  $-1$  or  $+1$ . For a small signal, this consumes far less power than a traditional two-level sigma-delta that must constantly switch between  $-1$  and  $+1$  such that the output average is nearly zero.

For the chosen process and the given load, the switch-mode output-stage power efficiency peaks at about 600 kHz. Given the clocks available, it was convenient to generate a 640-kHz clock. The response of the speaker being used rolls off quickly over 8 kHz and acts as the reconstruction filter for the sigma-delta DAC that gives us an effective over sampling ratio of 32.

Clock jitter modulates the pulse width of the DAC output stream, which causes high-frequency sigma-delta quantization noise to mix down into the baseband. Fig. 11 shows the simulated effects of clock jitter on dynamic range and input referred noise using nominal channel parameters,<sup>1</sup> which illus-

trates the importance of reducing clock jitter in the oscillator. With a fourth-order modulator, the overall noise performance of the DAC is limited by clock jitter and would not be improved by increasing the modulator order.

Return-to-zero (RTZ) coding is used to preserve linearity by improving the uniformity of the shape of the output pulses, which prevents high-frequency quantization noise from mixing down into the baseband. The RTZ pulse edges are resynchronized to the lowest jitter clock in the system just before feeding the output buffers, as shown in Fig. 12. This reduces sensitivity to jitter in the DAC circuitry and saves system power by requiring the supply current be spent only to suppress jitter in the clock oscillator core.

The three-stage ring oscillator shown in Fig. 13 provides a low-jitter clock. The bias current for all stages is trimmed at test to set the clock frequency to 2.56 MHz. The delay in each stage is implemented by symmetrical p and n transconductances and load resistances driving the gate capacitance of the next stage. Symmetry is essential to match clock waveform rise and fall times and reduce up-conversion of  $1/f$  noise [5]–[9]. In addition, extra capacitance added at the tail nodes  $C_T$  significantly reduces jitter from kickback and from current source noise. The bias current is digitally trimmed to set the oscillation frequency and is designed to vary linearly with temperature to reduce frequency variation over temperature.

<sup>1</sup>The nominal channel parameters are: ICL gain fixed at 34 dB,  $\alpha = 10$ ,  $\beta = 1/16$ ,  $\gamma = 1$ , and  $n = 1$ , giving a nominal channel gain of 31.5 dB at 5 kHz.

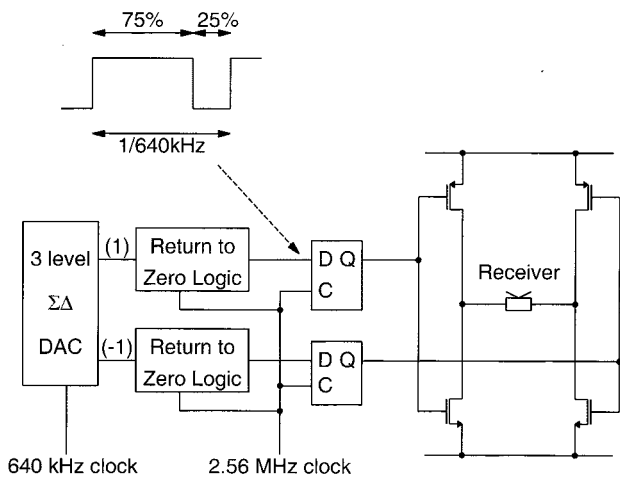


Fig. 12.  $\Sigma\Delta$  DAC and H-bridge timing.

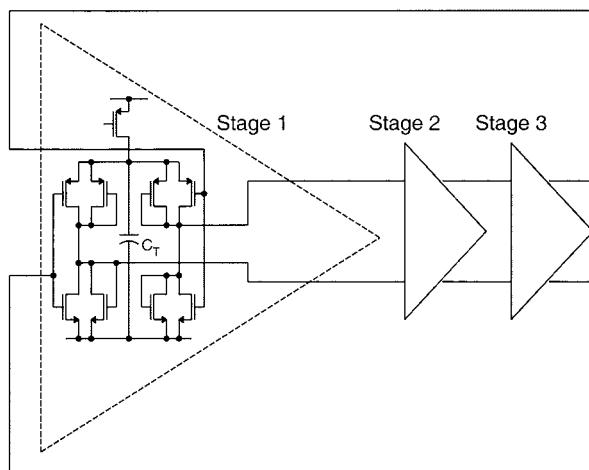


Fig. 13. Clock oscillator schematic.

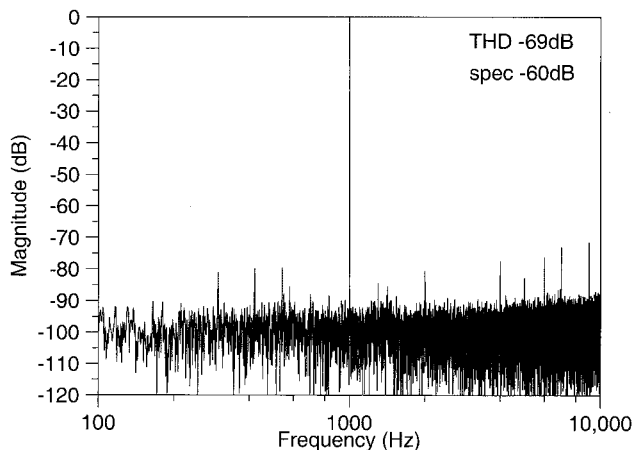


Fig. 14. Measured FFT response  $v_{in} = 4$  mV peak.

## VI. MEASURED RESULTS

A measured output voltage spectrum is plotted in Fig. 14. The input is a 1-kHz sinusoid at a 4-mV peak amplitude. The ICL has a gain of 50, making the 0-dB level 200 mV. This level corresponds to loud conversational speech at about 79 dB SPL and is 6 dB below the level where gain compression is initiated by the

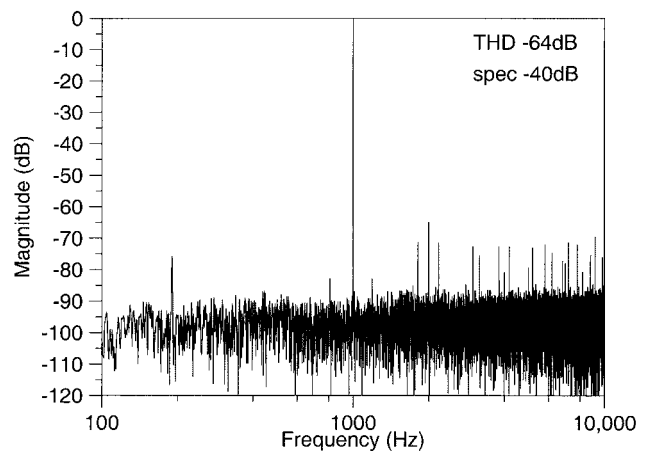


Fig. 15. Measured FFT response  $v_{in} = 80$  mV peak.

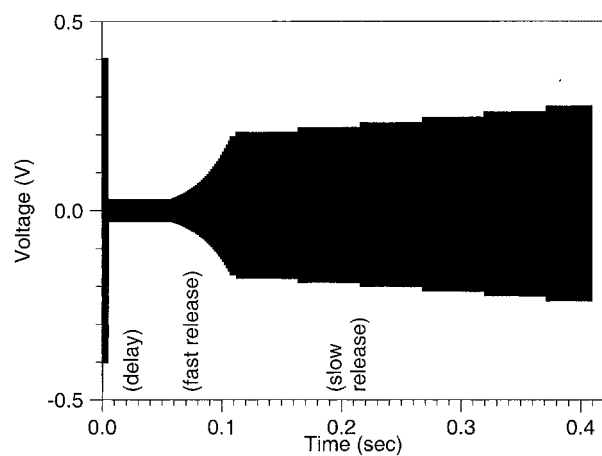


Fig. 16. Measured attack and release response for a short compression transient.

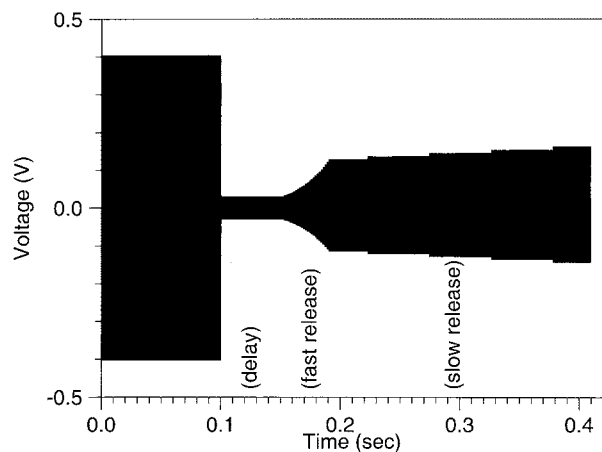


Fig. 17. Measured attack and release response for a long compression transient.

input stage. The output is loaded with a test circuit equivalent to the complex impedance of a receiver. Harmonic distortion at  $-69$  dB is well below the 0.1% specification for low-level inputs. Fig. 15 is the measured fast Fourier transform (FFT) response with an 80-mV peak amplitude at 1 kHz and input amplitude well into the compression region of the ICL circuit. With

TABLE I  
PERFORMANCE SUMMARY

Battery voltage range	1.1-1.5V
Battery current consumption (no signal)	
1.1V supply	
Analog	173 $\mu$ A
Digital	48 $\mu$ A
H-Bridge	15 $\mu$ A
Ring oscillator	34 $\mu$ A
Total	270 $\mu$ A
1.3V supply	299 $\mu$ A
1.5V supply	323 $\mu$ A
-3dB bandwidth	100Hz-10kHz
Input referred noise (100Hz-10kHz)	2.8 $\mu$ V <sub>RMS</sub>
Total harmonic distortion	
$V_{IN}=7$ mVpk	0.02%
$V_{IN}=80$ mVpk	0.5%
Input compressor maximum gain step error	0.09dB
Maximum input signal	450mV peak
Clock jitter	147ps RMS
Sub-bandgap reference stability	1%
Temperature range	20-40°C
Die size in 0.6 $\mu$ m, 3.3V CMOS	12mm <sup>2</sup>

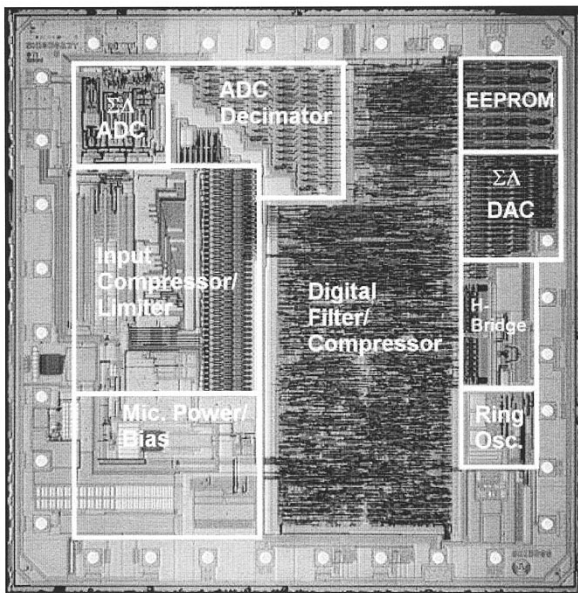


Fig. 18. Die micrograph.

an ICL gain of 50, this makes the 0-dB level equal to 800 mV in Fig. 15. The measured THD at -64 dB is well below the specification limit for the compression region. Figs. 16 and 17 show the release characteristics of the ICL. The output signal is shown when the input signal is suddenly decreased by 20 dB. The output initially drops 20 dB. After a short delay, the fast release shift register controls the compression and begins to increase the gain. Finally, the slow release shift register takes over and continues to increase the gain at a slower rate. The figures show that, for a longer time initially spent in compression, the fast release time is shorter and the slow release period starts at a lower gain and will take longer to get back to full gain. Table I summarizes the chip performance. Fig. 18 shows a microphotograph of the die.

## VII. CONCLUSION

A single-chip mixed-signal chip for a hearing aid instrument has been successfully implemented in a 0.6- $\mu$ m 3.3-V CMOS process. The typical input referred noise of the complete channel is 2.8  $\mu$ V<sub>rms</sub>. The typical total harmonic distortion of the complete signal channel is less than 0.02%. The IC consumes a total current of 270  $\mu$ A at 1.1 V and 299  $\mu$ A at 1.3 V. The complete chip, including bond pads, measures 12 mm<sup>2</sup>.

## ACKNOWLEDGMENT

The authors would like to express their gratitude to R. Garrison, M. Kennedy, T. Groller, P. Welsh, B. Rothbauer, M. Di-Cosmo, D. Hart, R. R. Dickerson, and K. Ling for their contributions on this project. In addition, they would like to thank L. Izzì and G. Frantz for their support. The authors would also like to thank the reviewers for their comments and suggestions.

## REFERENCES

- [1] H. Neuteboom, B. M. J. Kup, and M. Janssens, "A DSP-based hearing instrument IC," *IEEE J. Solid-State Circuits*, vol. 32, pp. 1790-1806, Nov. 1997.
- [2] J. W. Fattaruso *et al.*, "Analog processing circuits for a 1.1 V 270  $\mu$ A mixed signal hearing aid chip," in *IEEE Int. Solid-State Circuits Conf. (ISSCC)*, Feb. 2002, Session 23.3.
- [3] L. Williams, "Modeling and design of high-resolution sigma-delta modulators," Stanford University, Tech. Rep. ICL93-022, Aug. 1993.
- [4] "Hearing aid digital filter," U.S. Patent 6 292 571 B1, Sept. 18, 2001.
- [5] A. Hajimiri, S. Limotyrakis, and T. H. Lee, "Jitter and phase noise in ring oscillators," *IEEE J. Solid-State Circuits*, vol. 34, pp. 790-804, June 1999.
- [6] B. Razavi, "The study of phase noise in CMOS oscillator," *IEEE J. Solid-State Circuits*, vol. 31, pp. 331-343, Mar. 1996.
- [7] A. Hajimiri and T. H. Lee, "A general theory of phase noise in electrical oscillators," *IEEE J. Solid-State Circuits*, vol. 33, pp. 179-194, Feb. 1998.
- [8] T. H. Lee and A. Hajimiri, "Oscillator phase noise: A tutorial," *IEEE J. Solid-State Circuits*, vol. 35, pp. 326-336, Mar. 2000.
- [9] T. C. Wigandt, B. Kim, and P. R. Gray, "Analysis of timing jitter in CMOS ring oscillator," in *Proc. ISCAS*, 1994, pp. 27-30.

**D. George Gata** (M'86) received the B.A. (*magna cum laude*) degree in physics with a minor in mathematics and the M.S.E.E. degree in electrical engineering from Boston University, Boston, MA, in 1982 and 1985, respectively.

He served as a Member of the Technical Staff at AT&T Bell Labs from 1985 to 1989, first in the Transmission Systems Laboratory in North Andover, MA, working on long-haul digital microwave radio 64-QAM and 256-QAM ADC circuit packs and analog circuit SICs, then later in the Bipolar Circuits Lab based in Reading, PA, working on high-speed serial timing recovery products. In 1989, he joined Texas Instruments, Inc. (TI), as a Design Engineer and has worked in the mixed signal, wireless, broad-band, custom, and data acquisition areas where he has designed circuits for servo disc drives, V.90, high-performance audio, sigma-delta codecs, GSM, AMPS, and TDMA baseband wireless handsets, digital cameras, ADSL modems, VOIP cable modems, power conditioning, and hearing aids. He was the design leader of TI's SN105 023Y, or Songbird's SB15800 hearing aid IC project. Currently he is a Senior Member of the Technical Staff and Product Development Manager for the Low Power Codecs Group, Dallas, TX, in TI's High Performance Analog Data Acquisition SBE. He held a one-year IBM Predoctoral Graduate Research Fellowship in electrical engineering in 1984. He has four patents granted with four others pending. He serves as a member of the Industrial Advisory Council for the Electrical and Computer Engineering Department in Boston University's College of Engineering.

Mr. Gata was the Boston University Alumni Award Winner in physics in 1982. He has been a member of the IEEE Solid-State Circuits Society since 1986. He is a registered Professional Engineer in the state of Texas.

**Walter Sjursen** (S'76–M'77) received the B.S. degree in electrical engineering from Rutgers University, New Brunswick, NJ, in 1977 and the M.S. degree in engineering science from Pennsylvania State University, State College, in 1987.

He began his career in 1977 at Musitronics Corporation, Rosemont, NJ, where he designed audio signal processing circuits for musical instruments. Later in his career, he held engineering positions at a division of United Technologies Corporation, Fort Washington, PA, and later at Base Ten Systems, Inc., Trenton, NJ, where his designs involved digital circuits, video circuits, digital signal processing circuits, high-current control circuits, and a power converter for satellite applications. In 1995, he joined the David Sarnoff Research Center (now Sarnoff Corporation), Princeton, NJ, where he designed a 32-channel video A/D converter system for a custom high-speed CCD camera system, and low-power circuits to control electrochromic lens. Later at Sarnoff, he led the development of both analog and digital disposable hearing aids and was actively involved with the designs of the acoustics, transducers, and signal processing for the product. In 2001, he joined Songbird Hearing, Inc. (a spin-off company from Sarnoff to commercialize the disposable hearing aid), Cranbury, NJ, as the Director of Electroacoustics R&D where he continues to develop new hearing aid products. He holds 12 U.S. patents and has several patents pending.

Mr. Sjursen is a Member of Eta Kappa Nu, the Audio Engineering Society, the Acoustical Society of America, and the IEEE Solid-State Circuits Society.

**James R. Hochschild** (M'84) received the B.S. and M.S. degrees in electrical engineering from the University of Illinois in 1979 and 1981, respectively.

He joined Texas Instruments, Inc., Dallas, in 1980 where he has worked on the development of analog and digital telecommunication integrated circuits. He is currently involved in the development of low-power circuits for battery-operated systems.

**John W. Fattaruso** (S'75–M'84) received the B.S. (highest honors), M.S., and Ph.D. degrees in electrical engineering from the University of California, Berkeley, through 1986.

He has been a Hertz Foundation Fellow, Teaching Associate, Research Assistant, and Instructor at the University of California, Berkeley. In 1979 he worked in the Digital Signal Processing R&D Group at Hewlett-Packard, Santa Clara, CA, and in 1985 he served as a consultant to Seeq Technology, San Jose, CA. Since 1987, he has been with various research and product development departments of Texas Instruments Inc., Dallas, working on analog VLSI technology. He was elected a Distinguished Member of Technical Staff in 2001. His research interests include analog and RF circuit design, circuit simulation and optimization, neural networks and numerical analysis. He currently holds 23 patents in circuit design, has authored or coauthored 20 conference and journal papers, and has served on the analog program subcommittee of the ISSCC and as guest editor of the *Journal of Solid-State Circuits*.

Dr. Fattaruso is a member of Eta Kappa Nu, Tau Beta Pi, and Phi Beta Kappa.

**Lieyi Fang** (S'98–M'00) received the B.S. degree in acoustic electronics from Harbin Engineer University in 1982, the M.S. degree in biomedical engineering from Huazhong University of Science and Technology, China, in 1985, and Ph.D. degree in biomedical engineering from Chinese Academy of Sciences in 1992.

From 1997 he worked toward the Ph.D. in electrical engineering at Texas Tech University. From 1992 to 1993, he was an Assistant Professor/Associate Professor at Shanghai Institute of Physiology, Chinese Academy of Sciences. While at Texas Tech University Health Science Center (1994–1996) as a Research Associate, he was involved in vision research. In 1998, he joined Texas Instruments Inc., Dallas, as a Design Engineer. He was involved in the design and development of CCD AFE, analog video decoder AFE, high-speed data converter, PLL&DLL, oscillator, and sigma-delta modulator ADCs. His interests are in the design of high-speed data converters, high-frequency analog circuits, and sigma-delta modulator data converters. He has published over 30 publications and has several patents pending.

Dr. Fang was the co-recipient of Best Paper Award of ISPACS in 1999.

**Gerald R. Iannelli** received the B.S.E.E and M.S.E.E degrees from Drexel University, Philadelphia, PA, in 1984 and 1991, respectively.

He has held military-related positions at the Naval Air Development Center, Warminster, PA, RCA Missile and Surface Radar Division, Moorestown, NJ, and Philadelphia Naval Shipyard, where he received the U.S. Navy's Special Achievement Award for his work on naval ships. Between 1989 and 1995, he was a Senior Member, Engineering Staff at Matsushita Applied Research Laboratory, Burlington, NJ, where he focused on HDTV signal processing, video sample-rate conversion, and audio-for-video, doing the founding work for an Emmy award-winning product for Panasonic. In 1995, he joined Ensoniq Corp., Malvern, PA, as a Senior Project Engineer, where he led the design of professional digital music synthesizers and samplers. In 1997, he joined the Emmy award-winning Advanced Television Systems group of Sarnoff Corporation (formerly RCA David Sarnoff Research Center), Princeton, NJ, creators of the US HDTV Standard and Grand Alliance, where he was responsible for the first cross-country real-time transmission of HDTV over ATM networks. In 1998, he joined the Medical Systems Group as a key member of the Songbird Disposable Hearing Aid product development team. He is currently focused on audio signal processing, acoustics, and the design of other miniature healthcare devices. He holds one U.S. patent and has six pending.

Mr. Iannelli is a member of the Audio Engineering Society and Society of Motion Picture and Television Engineers.

**Zhongnong Jiang** received the B.S. degree in physics and M.S. degree in electrical engineering from Fudan University, Shanghai, China, in 1982 and 1985, respectively, and the Ph.D. degree in electrical engineering from the University of California, Los Angeles (UCLA), in 1995.

From 1991 to 1995, he was a Graduate Research Assistant in the Department of Electrical Engineering at UCLA, and his research interests are in the areas of speech/image encoding-decoding algorithms, digital filter design and parallel/pipelining architectures for digital signal processing. Since 1995, he has been at Texas Instruments, Inc., Dallas, and has been involved in developing several mixed-signal and digital signal processing IC products. He is now a Member of Group Technical Staff at Texas Instruments, Inc.

**Charles M. Branch** (M'95) received the B.S. and M.S. degrees in electrical and computer engineering from Carnegie Mellon University, Pittsburgh, PA, in 1995.

In 1995, he joined Texas Instruments, Inc., Dallas, in the Audio Design Group. Since then he has served in various IC design roles in mixed-signal, broad-band, and custom products. He has designed circuits in audio codecs, digital signal processors, ADSL codecs, power-line networking devices, digital hearing aids, and high-speed serial links. He is currently the Digital Design Applications and Flow Manager for Texas Instruments High Performance Analog Department. He has two patents pending.

Mr. Branch is a member of the IEEE Solid-State Circuits Society.

**James A. Holmes** received the B.S.E.E. and M.S.E.E. degrees from the University of Connecticut, Storrs, in 1990 and 1992, respectively.

In 1992 he joined Texas Instruments, Inc. (TI), Dallas, as a Mixed Signal CAD Methodologist. He has designed mixed-signal design methodologies and multi-level system simulation strategies and has written complex behavioral software models in a variety of computer languages and commercial CAD packages for various products across TI. He has been an invited speaker and published papers on mixed signal behavioral modeling and top-down IC design. He is currently a Member of Group Technical Staff on the Wireless Modeling Team in TI's Wireless Communications Business Unit.

**Michael L. Skorz** (S'84–M'86) received the B.S. degree in computer engineering from University of Illinois at Urbana in 1986.

He joined the Gould Research Lab in 1986 and worked as a parametric test engineer on a GaAs process development team. In 1988 he joined Monolithic Sensors Inc. (Knowles Electronics) as a device engineer working on CMOS process development, process characterization, SPICE modeling, and test development. He joined Texas Instruments, Inc. (TI), Dallas, in 1993 as a mixed-signal product and test engineer. Currently he is a Member of the Group Technical Staff at TI with expertise in mixed-signal test development and design-for-testability. His test development work has been applied on a wide range of mixed-signal products such as video RAMDACs, audio CODECs, custom SOCs, and most recently 802.11 WLAN base-band processors.



**Eugene (Gene) M. Petilli** received the M.S. degree in integrated electronics from Rochester Institute of Technology, Rochester, NY, in 1997.

From 1985 to 1997, he worked as a design engineer for Eastman Kodak, Rochester, specializing in high-speed image capture and full custom CMOS and BiCMOS mixed signal design. In 1997 he joined Intrinsic Corp., Westboro, MA, where he is the Technical Manager of the Mixed-Signal/RF ASIC Team. His interests include the design of sigma-delta data converters and integrated RF transceivers for wireless communications.

**Shuyou Chen** (M'97) received the B.S.E.E. degree from Harbin Engineering University, Harbin, China in 1987 and the M.S.E.E. degree from Rose-Hulman Institute of Technology, Terre Haute, IN, in 1996.

From 1987 to 1994, he worked as a Design Engineer with no. 707 Research Institute in Tianjin, China. From 1996 to 1998, he worked as a Staff Design Engineer with Iomega Corporation, San Diego, CA. He is currently a Senior Design Engineer with Texas Instruments, Inc., Dallas. He was involved in the design and development of low-power DSP and high-speed data communications chips such as IEEE-1394. His interests are high-speed/low-power digital/mixed-signal deep sub-micron ASIC/SoC, Networking and DSP/RISC processors.

Mr. Chen is a Member of the IEEE Computer Society.

**Gary Wakeman** was born in Lampasas, TX. He received the degree in drafting and design technology from American Trades Institute, Dallas, TX, in 1992.

He joined Clark IC Design, Dallas, TX in 1992 as a Contract Mask Layout Designer working on various mixed signal and analog IC layouts principally for Texas Instruments, Inc. In 1996, he joined Cyrix Inc. in their Microprocessor Group working on several microprocessor product layouts. In 1999, he went to work for Texas Instruments, Inc., Dallas, as a Senior IC Bar Designer in their Mixed Signal Custom Design Group working on various custom IC products. Currently he is with the Low Power Codecs Group in Texas Instrument's High Performance Analog Data Acquisition SBE.

**David A. Preves** (M'76) received the B.S. and M.S. degrees in electrical engineering from the University of Illinois and the Ph.D. degree in biomedical engineering from the University of Minnesota, Minneapolis.

He has over 25 years experience in technical project management at several hearing aid manufacturers. He holds nine patents in hearing aid technology and is chair of the ANSI working group on hearing aid measurements. He is currently a Senior Staff Engineer at Starkey Laboratories and Micro-Tech Hearing Instruments, Eden Prairie, MN.

**William A. Severin** was born in Bridgeport, TX, on September 9, 1955. He received the B.S.E.E. degree and the M.S.E.E. degree from Texas A&M University, College Station, in 1977 and 1983, respectively.

While in graduate school, his research was on the effects of a laser on the properties of semiconductor devices. He joined Texas Instruments, Inc. (TI), Houston, in 1979 and began working as a design engineer on telecommunications integrated circuits for TI terminal products. While in Houston, he was project leader for four CMOS IC modem designs and was promoted to manager of a design team in 1983. In 1986, he moved to TI in Dallas with his design team and joined the Mixed Signal Department of TI's Semiconductor Division as design section manager for telecommunications and analog interface circuits. He was made a Senior Member of the Technical Staff in 1987. He was promoted to design branch manager for telecommunications, wireless, and audio IC design in 1991 and was instrumental in developing TI's wireless baseband business. From 1997 to 2001, he was director of the design department for the Mixed Signal DSP Solutions Organization. In that role, he managed design teams that work on a variety of devices ranging from audio and video applications, modems, optoelectronics, speech and high-speed digital bus interfaces. Since 2001, he has been a key technical advisor on broadband solutions for high-speed data modems. He has also been active in university recruiting and relations teams, and is on the advisory board for the Electrical Engineering Department at Texas A&M University and is TI's representative to SRC Integrated Circuits and Systems Science Area. He holds five patents and has authored several articles on CMOS circuit design.